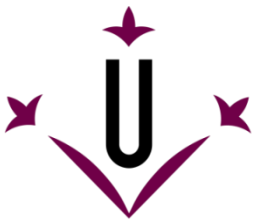

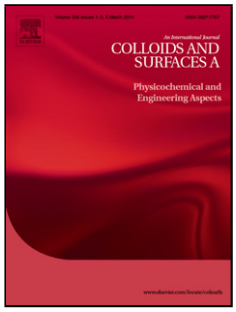

Title: Factors affecting the formation of highly concentrated emulsions and nanoemulsions

Authors: María Artiga-Artigas, Júlia Montoliu-Boneu, Laura Salvia-Trujillo, Olga Martín-Belloso

PII: S0927-7757(19)30561-8
DOI: https://doi.org/10.1016/j.colsurfa.2019.123577
Article Number: 123577

Reference: COLSUA 123577

To appear in: *Colloids and Surfaces A: Physicochem. Eng. Aspects*

Received date: 27 March 2019
Revised date: 17 June 2019
Accepted date: 17 June 2019

Please cite this article as: Artiga-Artigas M, Montoliu-Boneu J, Salvia-Trujillo L, Martín-Belloso O, Factors affecting the formation of highly concentrated emulsions and nanoemulsions, *Colloids and Surfaces A: Physicochemical and Engineering Aspects* (2019), https://doi.org/10.1016/j.colsurfa.2019.123577

Factors affecting the formation of highly concentrated emulsions and nanoemulsions

Authors:

Artiga-Artigas, María; Montoliu-Boneu, Júlia; Salvia-Trujillo, Laura & Martín-Belloso, Olga*.

Affiliations

Department of Food Technology University of Lleida – Agrotecnio Center Av. Alcalde Rovira Roure 191, 25198. Lleida, Spain

***e-mail corresponding author**: omartin@tecal.udl.cat

Garphical abstract

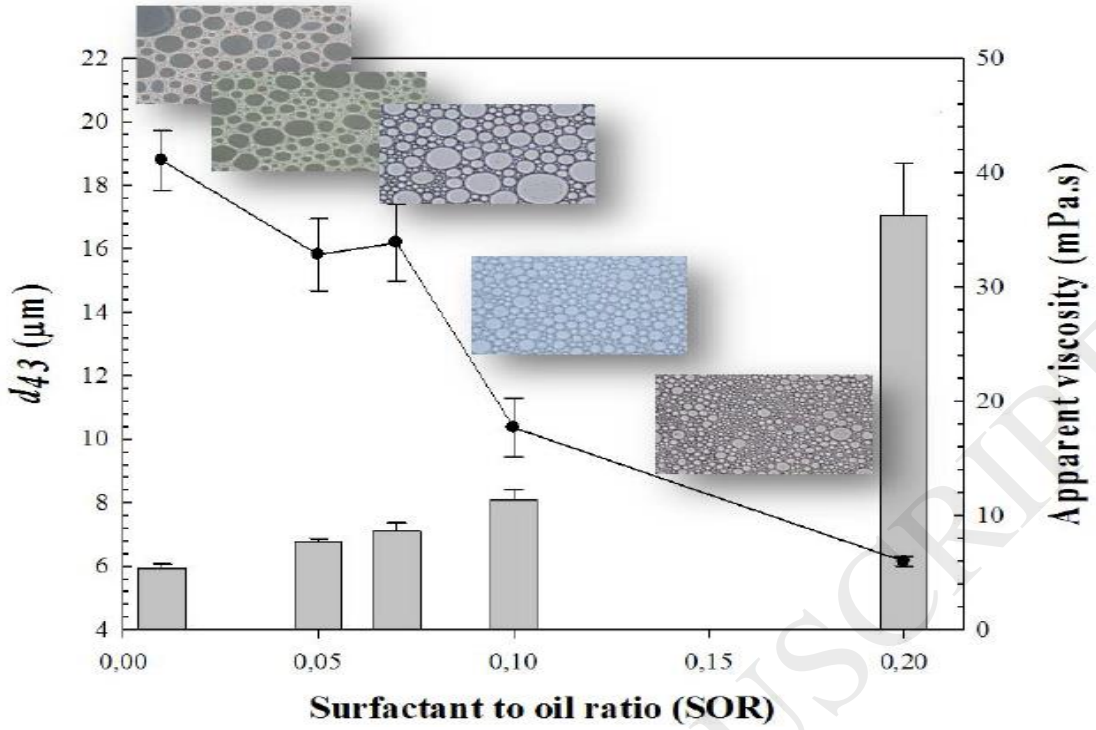

Abstract

Highly concentrated (HC) emulsions and or submicron emulsions arise as an interesting strategy to encapsulate and transport labile lipophilic bioactive compounds such as curcumin to be further incorporated into food formulations. The main factors affecting HC-emulsions formation and stabilization are the homogenization process, the oil volume fraction (φ) and the surfactant to oil ratio (SOR). Therefore, different HC emulsions were prepared by high-shear homogenization (HSH; 11,000 rpm, 2min), ultrasonication (US; 100 μm, 20-300 s) or microfluidization (MF; 800 bar, 1-5 cycles) varying the φ from 0.4 to 0.7 (40%-70% *w/w*) and the SOR from 0.01 to 0.2. HSH led to HC emulsions, whose particle sizes decreased from 14.46 to 2.42 μm (d_{43}), as the φ increased from 0.4 to 0.7. However, US and MF provoked the droplet breakup at oil concentrations over 50% *w/w*. Additionally, the higher the SOR at a fixed φ, the smaller

the particle size of the resultant HC emulsions regardless the homogenization procedure applied. Overall, particle size reduction produced a dramatic increase in emulsion viscosity due to a high packing state of droplets that in turn prevented droplets re-coalescence. Moreover, HC emulsions presented a high curcumin encapsulation efficiency (>70%) and release (> 80 % after 48 h is). Therefore, this work contributes to demonstrate that the small droplets size is governing the apparent viscosity in HC systems, as well as to elucidate the factors affecting their formation to be used as potential carriers of lipophilic bioactive compounds.

Keywords: highly-concentrated emulsions; nanoemulsions; curcumin; encapsulation efficiency; oil-volume fraction

1 Introduction

Recently, there is a strong interest in the design of emulsion-based structures as carriers of lipophilic bioactive compounds with numerous applications in the cosmetic, pharmaceutic and food industries. The control of the physicochemical and rheological properties of such emulsion-based systems is gaining attention in order to improve their processability, as well as the quality and functionality of the final products [1]. Highly concentrated (HC) emulsions also referred as high internal phase emulsions (HIPEs) or gel emulsions are defined as dispersed systems of two immiscible liquids, being O/W or W/O, with a volume fraction (φ) of the dispersed phase equal or higher than 0.4 (40 % *w/w*) [2,3]. The interest of O/W-HC emulsions as delivery systems rely on their capability to carry a high load of lipophilic compound per unit of emulsion volume due to their large oil concentration, thus being able to reduce storage and transport costs as well as allowing the oral administration of high doses of bioactive compounds in the

case of nutraceutical design [4]. For the formation of HC emulsions, the concentration of the dispersed phase may be increased up to a certain value considered as "critical" until the emulsion breaks or inverts [5]. Typically, this phenomenon occurs at dispersed φ equal or higher than 0.74 in monodisperse emulsions, when the dispersed droplets start losing their spherical shape and adopt a polyhedral shape due to the tight packing of the droplets [6]. Nevertheless, in polydisperse systems, the critical limit where emulsions present destabilization and subsequent breakage takes place at φ around 0.64 [1]. In this regard, the high droplet concentration and packing in HC emulsions leads to a significant impact on their rheological properties, changing from elastic to viscoelastic behavior due to the high increase in their apparent viscosity [7]. Therefore, the stabilization of HC emulsions affected by their physicochemical properties remains as a scientific challenge that needs elucidation.

In general, the formation of O/W emulsions is mainly affected by the oil droplet size regardless the dispersed phase concentration, which is in turn determined by the concentration of surfactant present in the system able to cover the interfacial area created during the emulsification process. In general, emulsions with smaller oil droplet sizes are more stable after their emulsification, presenting lower gravitation separation and aggregation in comparison with emulsions with larger oil droplet sizes [8]. There are several factors affecting the particle size of emulsions, being mainly the type and intensity of the homogenization method and the concentration of surfactant available in the system [9]. On the one hand, it is well-known that the application of high-shear forces through several homogenizing devices, namely high pressure homogenization or ultrasonication, is able to reduce the particle size of diluted emulsions, reaching the production of submicron nanoemulsions with oil droplet radii below 100 nm [9]. In fact, nanoemulsions, despite being thermodynamically unstable systems, present high kinetic

stability without droplet size changes during several months [10]. On the other hand, the higher the surfactant concentration the smaller the emulsion particle size, up to a minimum value where the oil/water interfacial area is saturated with surfactant molecules and an additional increase in surfactant concentration does not render smaller particles [11]. These principles have been well studied for emulsions with dispersed phase volumes up to 0.2 (20 % *w/w* of lipid phase) and could be applicable to enhance the stability of HC emulsions. However, the behavior of HC emulsions during emulsification may significantly differ from diluted emulsions [2]. Actually, the reduction of the particle size down to the nanometric range leads to a dramatic increase in the viscosity of emulsions [12–15], which in the case of HC emulsions may be even higher due to their high initial viscosity values. Therefore, the relationship between particle size reduction and emulsion formation in the case of HC emulsions needs to be studied.

Hence, the aim of the present work was to study the influence of the (*i*) emulsification method, being high shear homogenization (HSH), microfluidization (MF) or ultrasonication (US), and their respective processing parameters; (*ii*) oil volume fraction (φ = 0.4-0.7) and *(iii*) surfactant-to-oil ratio (SOR; 0.01-0.2) on the formation of HC emulsions in terms of their particle size and particle size distribution, ζ-potential, microstructure and apparent viscosity. Moreover, the use of HC emulsions as carriers of a lipophilic bioactive compound, being curcumin, was studied in terms of evaluating the curcumin encapsulation efficiency (EE in %) and its release kinetics in function of the emulsification method used.

2 Material and methods

2.1 Materials

Corn oil, purchased from (Koipesol Asua, Deoleo, Spain), was used as lipid phase for preparing all the emulsions. Tween 80 was purchased from Panreac (Barcelona, Spain) and used as surfactant. Ultrapure water obtained from a Milli-Q filtration system was used for the preparation of all solutions. Curcumin (*Curcuma longa*) was purchased from Sigma-Aldrich (Darmstadt, Germany). Ethanol absolute 99.9% purity (Fisher Chemical, Thermo Fisher Scientific, Leicestershire, UK) and n-hexane (≥ 95 % purity) (Scharlau, Scharlab S.L., Barcelona, Spain) were used as organic solvents.

2.2 Methods

2.2.1 Highly-concentrated emulsions formation

Overall, HC emulsions were formed by mixing the lipid phase, being corn oil, and the aqueous phase containing the hydrophilic surfactant with a T25 digital Ultra-Turrax (IKA, Staufen, Germany) at 11,000 rpm during 2 min. Then, the emulsification method and the processing parameters to prepare HC emulsions were evaluated as a first step. For this, the high-shear homogenization (HSH) was followed by 20-300 s of ultrasonication (US) at 100 µm of amplitude with a UP 400S Hielscher sonifier (Hielscher Ultrasound Technology, Teltow, Germany) or by 1-5 microfluidization (MF) cycles with a microfluidizer device (M110P, Microfluidics, Massachusetts, USA) working at 800 bar. Secondly, the effect of lipid phase concentration on the formation of HC emulsions was assessed by increasing the φ -calculated through eq.(1)- from 0.4 to 0.7. Finally, the impact of surfactant concentration on the physicochemical properties of the resultant HC emulsions was also studied by ranging the SOR from 0.01 to 0.2.

$$\varphi = \frac{C_{oil}}{C_{emulsion}} \qquad \textbf{eq.(1)}$$

where C_{oil} is the weight of oil expressed in *g* and $C_{emulsion}$ is the total weight of the emulsion also in g.

2.2.2 Physicochemical characterization of highly-concentrated emulsions

2.2.2.1 Droplet size and particle size distribution

The emulsion droplet size was measured by laser diffraction technique with a Mastersizer 3000^{TM} (Malvern Instruments Ltd., Worcestershire, UK) and was expressed in terms of volume and surface diameter (d_{43} and d_{32}, respectively) in µm. The refractive index of corn oil was 1.47. For the measurement of particle sizes HC emulsions were dispersed in distilled water using a dilution factor of 1:150 sample-to-water.

2.2.2.2 ζ-Potential

The ζ-potential (mV) was measured by phase-analysis light scattering (PALS) with a Zetasizer Nano-ZS laser diffractometer (Malvern Instruments Ltd, Worcestershire, UK). Samples were prior diluted in ultrapure water using a dilution factor of 1:150 sample-to-solvent.

2.2.2.3 Apparent Viscosity

Viscosity measurements (mPa·s) were performed by using a vibro-viscometer (SV-10, A&D Company, Tokyo, Japan) vibrating at 30 Hz, with constant amplitude and working at room temperature.

Aliquots of 10 mL of each HC emulsion or nanoemulsion were used for the determinations.

2.2.2.4 Emulsions microstructure

Phase contrast microscopy images of undiluted fresh HC emulsions were taken with an optical microscope (BX41, Olympus, Göttingen, Germany) equipped with UIS2

optical system. All images were processed using the instrument software (Olympus cellSense, Barcelona, Spain).

2.2.3 Curcumin encapsulation in highly-concentrated emulsions

For the enrichment of corn oil with curcumin, the oil was heated at mild temperature (50 ºC) and mixed with 0.01% *w/w* curcumin powder for 10 minutes of magnetic stirring followed by 5 minutes of sonication in an ultrasonic bath (J.P Selecta, Barcelona, Spain) ensuring its complete dissolution. Afterwards, high-shear homogenized (HSH-) emulsions and their respective ultrasonicated (US-) or microfluidized (MF-) emulsions (SOR=0.1 and φ=0.5) were prepared as mentioned in section 2.2.1. These emulsions were characterized in terms of particle size, ζ-potential and apparent viscosity as described in section 2.2.2. Moreover, the encapsulation efficiency (EE) and the curcumin release both expressed in percentage were also assessed.

2.2.3.1 Encapsulation Efficiency

The concentration of curcumin loaded in the HC emulsion was determined following the method proposed by Lin et al. (2018). In this method, 0.5 mL of each HC emulsion is poured in a solution containing 2 mL of ethanol absolute and 3 mL of n-hexane, and vortexed (MS2, Fisher Scientific, Leicestershire, UK). Curcumin was collected in the ethanol fraction and subsequently quantified. Its absorbance was measured with a V-670 spectra photometer (Jasco, Tokyo, Japan) at a wavelength of 425 nm and the concentration was obtained from the calibration curve. Afterwards, encapsulation efficiency (EE, %) of the obtained emulsions was calculated by eq.(2):

$$\%EE = \frac{Total\ amount\ of\ curcumin - Free\ curcumin}{Total\ amount\ of\ curcumin} \text{x } 100 \qquad \textbf{eq.(2)}$$

where the total amount of curcumin is the initial concentration of the bioactive compound added to the mixture and the free curcumin is the concentration not loaded in the highly concentrated emulsion.

2.2.3.2 Curcumin release

Aliquots of 10 mL of HC emulsion loaded with curcumin were placed inside a dialysis tubing cellulose membrane of 43 mm x 27 mm (Sigma-Aldrich, Darmstadt, Germany) and submerged in 20 mL of food grade ethanol. Curcumin release was measured during 0.5, 1, 3, 5, 8, 24 and 48 h following the method described by Behbahani, Ghaedi, Abbaspour, & Rostamizadeh (2017). The released curcumin was quantified spectrophotometrically with a V-670 spectrophotometer (Jasco, Tokyo, Japan) at 425 nm. The curcumin release was calculated with eq.(3):

$$Release\ (\%) = \frac{C_r}{C_t} x100 \qquad \textbf{eq.(3)}$$

where C_r is the released curcumin expressed in mg being the amount of curcumin found in each sample and C_t is the total amount of encapsulated curcumin that was loaded in the highly concentrated emulsions according to encapsulation efficiency results, also expressed in mg.

The curcumin release curve over 24 hours showed a steep increase at short time until reaching a plateau phase fitting a fractional conversion model to describe the relationship between *CR* and t independent variables as shown in eq.(4). Curcumin release was modeled by a fractional conversion method using JMP 12 Pro 12 software (Statistical Discovery™, North Carolina, USA).

$$CR = CR_{max} \cdot (1 - e^{-kt}) \quad \textbf{eq.(4)}$$

where *CR* is the curcumin release expressed in %, t is the time (h), CR_{max} is the maximum estimated curcumin release (%) and k is the kinetic constant (h^{-1}).

2.2.4 Statistics

All the experiments were assayed in duplicate, and at least three replicate analyses were carried out for each parameter. JMP Pro 12 software (Statistical Discovery™, North Carolina, USA) was used to perform the statistical analysis. Tukey-Kramer test was chosen to determine significant differences among treatments, at a 5% significance level.

3 Results and discussion

Throughout this manuscript, the effect of *(i)* the homogenization method of HC emulsions preparation (*i.e.* high-shear homogenization, ultrasonication and microfluidization), *(ii)* the influence of φ and *(iii)* the SOR, on the droplet size and droplet size distribution, viscosity, ζ-potential and microstructure of the resultant HC emulsions has been addressed. Additionally, their capacity as delivery systems of curcumin was also assessed.

3.1 Effect of emulsification method on the physicochemical characteristics of HC emulsions

The influence of the emulsification method on the formation of HC emulsions was evaluated maintaining the oil volume fraction at 0.4 and the SOR at 0.1 while

varying the US processing time (s) working at an amplitude of 100 μm and the number of cycles of MF at 800 bar, respectively. Subsequently, their particle size and particle size distribution and ζ-potential was determined (Figure 1). Emulsions prepared by HSH (11,000 rpm, 2 min) had a volume mean droplet diameter (d_{43}) of 14.46 ± 1.87 μm and exhibited a bimodal particle size distribution with a major intensity peak with particles larger than 10 μm. The particle size of HC emulsions significantly decreased after applying both US or MF treatments at increasing the intensity of the homogenization method, reaching the formation of submicron emulsions (Figure 1). In fact, a gradual displacement of the main intensity peaks towards the nanorange was observed in the particle size distribution, reaching monomodal particle size distributions after 200 s of US (Figure 1A). On the one hand, the average droplet size (d_{43}) of ultrasonicated (US) emulsions gradually decreased from 13 ± 1 μm down to 0.65 ± 0.03 μm at increasing sonication time from 20 to 200s (Figure 1B). Nonetheless, the droplet sizes (d_{43} and d_{32}) and the particle size distribution of HC emulsions did not show a significant decrease after the application of US treatment beyond 200 s (Figure 1A-B). Salvia-Trujillo, Rojas-Graü, Soliva-Fortuny, & Martín-Belloso (2013) reported that ultrasounds were a feasible technology to produce diluted nanoemulsions (1% *w/w* lipid phase) with particles sizes lower than 100 nm since cavitation forces generated by the sonicator can induce disruption at droplets interface producing stable nanoemulsions. Nonetheless, at higher oil droplet concentration present in HC emulsions may diminish the efficiency in particle size reduction by US in comparison with diluted emulsions, probably due to (*i*) a lower energy input per unit of dispersed phase, or to (*ii*) a greater extent of coalescence caused by higher collision frequency of oil droplets [4,7].

On the other hand, MF led to the formation of submicron emulsions with d_{43} below 0.6 ± 0.02 μm and monomodal distributions after the first cycle (Figures 1D and E,

respectively). The observed differences in the particle size of submicron emulsions depending on the applied emulsification method could be related to technological differences between the ultrasonicator and the microfluidizer [9]. Therefore, high shear stress produced inside the microfluidizer channels can lead to more homogeneous emulsions with lower particle sizes than high shear mixers and ultrasonicators [19]. Moreover, HC nanoemulsions reached a particle size of 0.346 ± 0.003 μm after two cycles of MF, with a negligible decrease during the following cycles (Figure 1D). Likewise, other works also suggest that a further increase in the number of cycles do not lead to a significant reduction of the average droplet size provided that droplets have reached their saturation size [20]. Indeed, interdroplet forces generated in HC systems due to their oil droplets compacted structure, which are responsible for stabilizing droplets against coalesce, may counteract the compression and tension forces created inside the homogenization devices diminishing their efficiency [1].

The ζ-potential of HC emulsions treated by HSH was negative, with a value of -38 ± 2 mV at neutral pH conditions (pH ≈6). Despite that Tween 80, used as surfactant in this study, is considered a non-ionic surfactant, it has been consistently observed that it may provide negative charge to emulsions and nanoemulsions [21]. In agreement to this, it has been reported that OH^- ions from the aqueous phase or HCO_3^- and CO_3^{2-} ions from the dissolved atmospheric CO_2 may be oriented towards the oil/water interface thus conferring negative charge to oil droplets [22]. It was observed that an increase in the time of US treatment or the number of cycles through the microfluidizer led to less negative ζ-potential values in HC emulsions, reaching values of -26 ± 2 mV or to -22 ± 4 mV in the case of US- or MF-emulsions, respectively (Figures 1C or 1F, respectively). It has been described that during homogenization processes such as US or

MF, Tween 80 molecules are better displaced and arranged at the oil/water interface, thus contributing in reducing the negative charge [23,24].

3.2 Influence of oil volume fraction on the physicochemical characteristics of HC emulsions

HC emulsions with φ between 0.4 and 0.7 were prepared by three different emulsification methods: HSH (11,000 rpm, 2 min); HSH followed by US (100 μm, 200 s) or HSH followed by MF (800 bar, 2 cycles). The increase of the φ from 0.4 to 0.7 had a different effect on the particle size of the resultant HC emulsions depending on the homogenization method applied (Figure 2A-C).

In the HSH-treated HC emulsions, the particle size decreased from 14.46 ± 2.13 to 2.42 ± 0.01 μm as increasing the φ from 0.4 to 0.7 (Figure 2A). This particle size decrease was visually observed in the microscopy images, where a clear particle size reduction was detected when increasing the oil droplet concentration at constant HSH treatment conditions (Figure 3 A, D, G, J and M). This phenomenon might be related to the fact that a higher oil concentration can lead to the placement of oil droplets closer together thus increasing their packing state. In turn, the droplets packing may contribute to avoid or prevent droplets re-coalescence after emulsification thus rendering a smaller particle size, which is in agreement with particle size distributions shown in Figure 2A. This has been previously reported by other authors, who established that the increase in the lipid phase concentration led to smaller oil droplet sizes being attributed to their higher stress forces created during emulsification [25]. Additionally, the reduction of HSH-treated emulsions' particle size caused the rise of their apparent viscosity, which increased from 6.13 ± 0.73 to 624 ± 21 mPa·s when the φ incremented from 0.4 to 0.7 (Figure 4A). In fact, the most pronounced viscosity increase (approximately 5 times) was observed when rising the φ from 0.6 to 0.65 or from 0.65 to 0.7. According to this,

an increase in the dispersed phase concentration, which in this case is the oil phase, obviously leads to an increase in the apparent viscosity of emulsions. Nonetheless, the particle size reduction as a consequence of the dispersed phase concentration may have significantly contributed in the apparent viscosity increase. In fact, at constant φ, the number of dispersed particles (droplets) will increase when particle size decreases, which in turn may cause a higher packing state of droplets [26], thus explaining the dramatic increase of emulsions' apparent viscosity at higher φ. As a result, the number of interactions between particles might increases as well, leading to an overall increase in viscosity [27].

In contrast, in US- and MF-treated emulsions, the higher the φ, the larger the emulsion particle size (Figures 2B and 2C, respectively). This opposite tendency between HSH-emulsions and US or MF-emulsions might be explained by the differences in each of the devices during emulsification. In US or MF devices, the breaking of submicron droplets in the flow field may induce coalescence between the highly deformed droplets [28]. This can be also perceived in the microscopic images corresponding to US- and MF- emulsions containing a φ over 0.6, where an increase in droplets particle size was observed suggesting the destabilization of the system after emulsification (Figure 3H, K, N and 4I, L, respectively). Therefore, the higher the φ, the greater feasibility to provoke droplets coalescence in HC emulsions. In fact, emulsions with 0.7 φ were completely destabilized after the application of US emulsification treatment, reaching particle size values of 30.85 ± 1.12 μm (Figure 2B). A similar behavior was observed in MF-emulsions, which suffered fast coalescence and subsequent phase separation after the first cycle when the φ was 0.6 or 0.65 (Figure 2C). Moreover, both for US or MF-treated emulsions, increasing the oil concentration rendered emulsions with larger particle size and with a higher apparent viscosity

(Figures 4B and 4C). In addition, increasing the dispersed phase concentration above 0.65 and 0.5 in US and MF respectively caused the emulsion breaking and the subsequent fall of their apparent viscosity (Table 1) due to the complete separation of the lipid and aqueous phases. Furthermore, at the same φ, the apparent viscosity of US- and MF-emulsions was higher than that of HSH-emulsions. This phenomenon can be explained due to the submicron particle size of US- and MF-emulsions. According to Luckham & Ukeje (1999), small droplets can fit into the gaps between large droplets reducing particles interactions and losing the viscoelasticity previously acquired by the high oil concentration. Therefore, HC submicron emulsions have similar viscosity values than emulsions with larger droplet size yet using lower concentrations of the lipid phase, which might be an advantage when formulating low fat emulsions.

The ζ-potential of all the prepared HSH-emulsions and submicron emulsions was negative but varied depending on the homogenization process applied (Table 1). HSH-emulsions showed ζ-potential values around -40 mV regardless the φ. Oppositely, in US- and MF-emulsions the ζ-potential was less negative than in the case of those HSH-presenting values around -30 mV. In addition, in this case, the ζ-potential depended on the φ, becoming less negative as increasing the oil concentration before the breaking of emulsions' structure (Table 1). Actually, ζ-potential of US-emulsions incremented from -26 to -20 mV when the φ increased from 0.4 to 0.6 (Table 1). Then, the ζ-potential decreased again reaching values even more negative than the initial ones (-37.0 ± 2.6 mV). This jump corresponded with the destabilization of the US-emulsions (φ > 0.6) suggesting that ζ-potential is closely related to the particle size. The decrease in particle size of HC emulsions induced by the increase of the φ favors the location of surfactant around oil droplets. Therefore, as has been discussed in section 3.1 the smaller the

particle size, the Tween 80 locates itself better at droplets interface neutralizing the interfacial charge.

3.3 Impact of surfactant concentration on the physicochemical characteristics of highly concentrated emulsions

Based on the results prior discussed, φ was fixed at 0.5 since HC emulsions containing this φ could be processed by the three emulsification methods (HSH, US or MF). Subsequently, the influence of increasing the SOR from 0.01 to 0.2 on the formation of HC emulsions was evaluated. The particle size of all the prepared HC HSH- (11,000 rpm, 2 min), US- (200 s, 100 μm) and MF- (2 cycles, 800 bar) emulsions decreased at increasing the SOR from 0.01 to 0.2 (Figures 5A-C). Indeed, regarding HSH-emulsions, the particle size in terms of d_{43} decreased from 18.66 ± 0.95 down to 6.72 ± 0.16 μm at increasing the SOR from 0.01 to 0.2 (Figure 5A). In general, it is known that higher surfactant concentrations facilitates the oil droplet disruption during emulsification and allows a faster coverage of the oil droplet coverage, thus rendering emulsions with smaller particle sizes [4,30]. Therefore, the concentration of surfactant may influence the formation of HC emulsions since an increase of Tween 80 concentration led to HC emulsions with smaller particle sizes, which favors its stability over time [31]. Moreover, HSH-treated emulsions exhibited bimodal particle size distributions regardless the SOR and significant differences were not observed for those with a SOR of 0.05 and 0.07 (Figure 5A). In contrast, after US or MF, all the submicron emulsions prepared with an SOR greater or equal to 0.05 presented smaller particle sizes than those treated by HSH and monomodal particle size distributions (Figures 5B-C). This can be explained since US and MF are more efficient techniques than HSH to minimize the particle size leading to more homogeneous particle size distributions [1].

Furthermore, microscopic images of emulsions showed an increase in the droplet packing and consequently a reduction in their particle size at increasing surfactant concentrations regardless the emulsification treatment applied (Figure 6). The microscopic image of HSH-emulsion with a SOR of 0.2 (Figure 6M) exhibited a high packing of droplets likewise those US-emulsions (Figure 6N). Unlike HSH-treated emulsions and US-, MF-emulsions were undetectable by optical microscopy, regardless their SOR due to that droplet sizes were below the detection limit of the device, being below 3 μm (Figure 6O). In fact, the achievement of such small particle sizes involves a very high packing of the droplets, which may suppress droplets collisions and subsequent coalescence, thus rendering smaller particle sizes [1].

The decrease in droplet size in turn contributed to increase the apparent viscosity of emulsions regardless the emulsification method applied (Figure 7A-C). Nevertheless, the most dramatic increase in the apparent viscosity in HC emulsions was observed when they were treated by MF. In fact, in MF-treated emulsions increasing the SOR from 0.1 to 0.2 led to a particle size reduction from 360 nm down to 240 nm, yet it led to an apparent viscosity increase from 69 to 638 mPa.s. This means that a reduction in the oil droplet size of aproximately 100 nm leads to a 10-fold increase in the apparent viscosity of the HC emulsions. The dramatic increase in the apparent viscosity of those HC emulsions with a SOR of 0.2, can be attributed to their nanometric particle size since unlike section 3.2, in this experimental section the dispersed phase concentration remained constant. This suggests that the particle size governs the apparent viscosity of HC emulsions.

HSH-emulsions and submicron emulsions showed negative ζ-potential values regardless the concentration of surfactant (Table 2). According to our results, the tendency of ζ-potential was to move towards less negative values in all the types of

emulsions (HSH, US or MF). Nevertheless, the ζ-potential of HSH and submicron emulsions were significantly different ($p<0.05$) among them becoming less negative after ultrasonication or microfluidization process (Table 2). Actually, HSH-emulsions presented values ranging from -52.6 ± 3.7 to -37 ± 3 mV as increasing the SOR from 0.01 to 0.2, respectively. Regarding the ζ-potential of submicron emulsions, it was approximately between -42 ± 2 and -24 ± 4 mV at the same surfactant concentration. Indeed, US or MF reduced emulsion particle size contributing to increase the surface area available to be covered by Tween 80. Hence, there will be less non-adsorbed surfactant molecules in the continuous phase making the ζ-potential less negative [32].

3.4 Encapsulation efficiency and curcumin release kinetics of highly-concentrated emulsions

HC emulsions (HSH-, US- and MF-) loaded with curcumin were prepared fixing the φ at 0.5 and the SOR at 0.1. All of them presented encapsulation efficiencies (EE) greater than 70%. Nonetheless, significant differences were observed depending on the type of the emulsification method. In fact, HC emulsion prepared by HSH (11,000 rpm, 2 min) exhibited the highest EE with a value of 78 ± 3%, whereas those US- (100 μm, 200 s) or MF- (800 bar, 2 cycles) showed EE of 72.4 ± 1.8 or 71.21 ± 0.01%, respectively. Differences might be due to the curcumin degradation through the cavitation or high pressure forces from the ultrasonicator or microfluidizer, respectively. Curcumin is prone to suffer auto-oxidation when it is exposed to the aqueous media due to its instability leading to the formation of degradation products [33]. HC emulsions subjected to US reached temperatures over 60 ºC at the outlet of the processing equipment. Therefore, this temperature might be locally even higher inside the ultrasonic treatment chamber generating species such as hydrogen peroxide able to

accelerate the oxidation of curcumin. In fact, Riesz, Berdahi, & Christman (1985) reported that cavitation phenomena induced by ultrasounds produce the collapse of air bubbles within the fluid. This causes a local increase of the pressure and temperature, which in turn results in the dissociation of water into hydroxyl radicals and hydrogen atoms, appearing several molecular species in the media such as hydrogen peroxide [35]. Further research also supported that high shear forces such as those inside the microfluidizer may lead to high energy molecules like hydroxyl radicals, which can cause chemical degradation [36].

Curcumin release kinetics during 48h is shown in Figure 8 along with their kinetic parameters including the maximum estimated curcumin release (CR_{max}) and the kinetic constant (k). Concerning the calculated kinetic parameters yielded by the adjusted model showed in eq.(3), neither the CR_{max} values (>80%) nor k values (≈0.031 h^{-1}), were significantly different regardless the type of HC emulsion. Moreover, HSH-, US- and MF-emulsions were able to release more than the 60% of the curcumin amount after 48h of experiment. This suggested that all the prepared HC emulsions resulted efficient as carriers and delivery systems of curcumin regardless the homogenization method used for their preparation. Furthermore, since d_{43} of HSH-, US- and MF- emulsions was completely different (11.2, 0.46 and 0.36 μm, respectively), it can be determined that particle size did not affect the release rate.

4 Conclusions

Either HSH (11,000 rpm, 2 min) alone or followed by US (200 s, 100 μm) or MF (2 cycles, 800 bar) allowed the preparation of HC emulsions. On the one hand, the increase of the φ contributed to reduce the particle size of HSH-emulsions regardless the processing conditions applied. This particle size reduction immediately provoked the increase of HSH-emulsions' apparent viscosity due to the great droplet packing. Oppositely, US- and MF-emulsions with an φ over 0.5 suffered coalescence after emulsification since cavitation and high-shear forces caused their over-processing. On the other hand, it was observed that for a fixed oil concentration, the particle size of HC emulsions decreased as the SOR increased from 0.01 to 0.2 regardless the emulsification method used. However, US and MF led to HC submicron emulsions (φ = 0.5) with particle sizes lower than 500 nm when the SOR was at least 0.1. For this reason, the sharp increase of HC emulsions' apparent viscosity was even higher after US or MF than in the case of HSH due to the presence of submicron particles. This showed that, in fact, the increase of apparent viscosity is strongly determined by the decrease in particle size. Our results evidence that HC emulsions with particle sizes in the nanometer range (≈ 200 nm) present much higher viscosity values in comparison with emulsions with larger particle sizes, which may be interesting for the development of emulsified systems with specific rheological characteristics using lower dispersed phase concentrations. Moreover, all the emulsion-based HC systems prepared during the present study showed a high capability for the encapsulation and release of curcumin according to their kinetic constants. Therefore, the present work contributes to comprehend the role of particle size reduction on the formation of HC emulsions and the effect of the emulsification method, φ and SOR on their final emulsion characteristics allowing the preparation of HC nanoemulsions. The study of these parameters is of great importance in order to design emulsion-based nanostructures with

controlled characteristics, especially with highly concentrated phases, to be used as efficient delivery systems of bioactive compounds.

5 Acknowledgments

This study was funded by the Ministry of Economy, Industry and Competitiveness (MINECO/FEDER, UE) throughout project **AGL2015-65975-R**. María Artiga-Artigas thanks the University of Lleida for her pre-doctoral fellowship. Laura Salvia-Trujillo thanks the "Secretaria d'Universitats i Recerca del Departament d'Empresa i Coneixement de la Generalitat de Catalunya" for the Beatriu de Pinós post-doctoral grant (**BdP2016-00336**).

6 References

[1] R. Foudazi, S. Qavi, I. Masalova, A.Y. Malkin, Physical chemistry of highly concentrated emulsions, Adv. Colloid Interface Sci. 220 (2015) 78–91.

[2] L. Bai, S. Huan, J. Gu, D. Julian, Food Hydrocolloids Fabrication of oil-in-water nanoemulsions by dual-channel micro fl uidization using natural emulsi fi ers : Saponins , phospholipids , proteins , and polysaccharides, Food Hydrocoll. 61 (2016) 703–711.

[3] R.H. Muller, D. Harden, C.M. Keck, Development of industrially feasible concentrated 30% and 40% nanoemulsions for intravenous drug delivery, Drug Dev. Ind. Pharm. 38 (2012) 420–430.

[4] X. Luo, Y. Zhou, L. Bai, F. Liu, R. Zhang, Z. Zhang, B. Zheng, Y. Deng, D.J. McClements, Production of highly concentrated oil-in-water emulsions using dual-channel microfluidization: Use of individual and mixed natural emulsifiers (saponin and lecithin), Food Res. Int. 96 (2017) 103–112.

[5] H.M. Princen, M.P. Aronson, J.C. Moser, Highly Concentrated Emulsions, J. Colloid Interface Sci. 75 (1980) 246–270.

[6] N.N. Tshilumbu, E.E. Ferg, I. Masalova, Instability of highly concentrated emulsions with oversaturated dispersed phase. Role of a surfactant, Colloid J. 72 (2010) 569–573.

[7] G. Calderó, A. Patti, M. Llinàs, M.J. García-Celma, Diffusion in highly concentrated emulsions, Curr. Opin. Colloid Interface Sci. 17 (2012) 255–260.

[8] D.J. McClements, Edible nanoemulsions: fabrication, properties, and functional performance, Soft Matter. 7 (2011) 2297–2316.

[9] L. Salvia-Trujillo, M.A. Rojas-Graü, R. Soliva-Fortuny, O. Martín-Belloso, Impact of microfluidization or ultrasound processing on the antimicrobial activity against Escherichia coli of lemongrass oil-loaded nanoemulsions, Food Control. 37 (2014) 292–297.

[10] M.I. Guerra-Rosas, J. Morales-Castro, L.A. Ochoa-Martínez, L. Salvia-Trujillo, O. Martín-Belloso, Long-term stability of food-grade nanoemulsions from high methoxyl pectin containing essential oils, Food Hydrocoll. 52 (2016). doi:10.1016/j.foodhyd.2015.07.017.

[11] A. Zdziennicka, K. Szymczyk, J. Krawczyk, B. Jańczuk, Critical micelle concentration of some surfactants and thermodynamic parameters of their micellization, Fluid Phase Equilib. 322–323 (2012) 126–134.

[12] O. Sonneville-Aubrun, J.T. Simonnet, F. L'Alloret, Nanoemulsions: A new vehicle for skincare products, Adv. Colloid Interface Sci. 108–109 (2004) 145–149.

[13] R. Pal, Effect of Droplet Size on the Rheology of Emulsions, AIChE J. 42 (1996) 3181–3190.

[14] T. Tadros, P. Izquierdo, J. Esquena, C. Solans, Formation and stability of nano-emulsions, Adv. Colloid Interface Sci. 108–109 (2004) 303–318.

[15] T.G. Mason, J.N. Wilking, K. Meleson, C.B. Chang, S.M. Graves, Nanoemulsions: formation, structure, and physical properties, J. Phys. Condens. Matter. 18 (2006) R635–R666.

[16] C. Lin, X. Zhang, H. Chen, Z. Bian, G. Zhang, M.K. Riaz, D. Tyagi, G. Lin, Y. Zhang, J. Wang, A. Lu, Z. Yang, Dual-ligand modified liposomes provide effective local targeted delivery of lung-cancer drug by antibody and tumor lineage-homing cell-penetrating peptide, Drug Deliv. 25 (2018) 256–266.

[17] E.S. Behbahani, M. Ghaedi, M. Abbaspour, K. Rostamizadeh, Optimization and characterization of ultrasound assisted preparation of curcumin-loaded solid lipid nanoparticles: Application of central composite design, thermal analysis and X-ray diffraction techniques, Ultrason. Sonochem. 38 (2017) 271–280.

[18] L. Salvia-Trujillo, A. Rojas-Graü, R. Soliva-Fortuny, O. Martín-Belloso, Physicochemical Characterization of Lemongrass Essential Oil-Alginate Nanoemulsions: Effect of Ultrasound Processing Parameters, Food Bioprocess Technol. 6 (2013).

[19] J. Bonilla, L. Atarés, M. Vargas, A. Chiralt, Effect of essential oils and homogenization conditions on properties of chitosan-based films, Food Hydrocoll. 26 (2012) 9–16.

[20] T.J. Wooster, M. Golding, P. Sanguansri, Impact of oil type on nanoemulsion formation and ostwald ripening stability, Langmuir. 24 (2008) 12758–12765.

[21] L. Salvia-Trujillo, A. Rojas-Graü, R. Soliva-Fortuny, O. Martín-Belloso, Physicochemical characterization of lemongrass essential oil-alginate anoemulsions: effect of ultrasound processing parameters, Food Bioprocess Technol. 6 (2013) 2439–2446.

[22] K.G. Marinova, R.G. Alargova, N.D. Denkov, O.D. Velev, D.N. Petsev, I.B. Ivanov, R.P. Borwankar, Charging of Oil−Water Interfaces Due to Spontaneous

Adsorption of Hydroxyl Ions, Langmuir. 12 (1996) 2045–2051.

[23] L. Salvia-Trujillo, E.A. Decker, D.J. McClements, Influence of an anionic polysaccharide on the physical and oxidative stability of omega-3 nanoemulsions: Antioxidant effects of alginate, Food Hydrocoll. 52 (2016) 690–698.

[24] T.D. Dimitrova, F. Leal-Calderon, Forces between emulsion droplets stabilized with Tween 20 and proteins, Langmuir. 15 (1999) 8813–8821.

[25] M. Briceño, J.L. Salager, J. Bertrand, Influence of dispersed phase content and viscosity on the mixing of concentrated oil-in-water emulsions in the transition flow regime, Chem. Eng. Res. Des. 79 (2001) 943–948.

[26] H.C. Brinkman, The viscosity of concentrated suspensions and solutions, J. Chem. Phys. 20 (1952) 571.

[27] I.M. Krieger, T.J. Dougherty, A Mechanism for Non-Newtonian Flow in Suspensions of Rigid Spheres, Trans. Soc. Rheol. 3 (2002) 137–152. doi:10.1122/1.548848.

[28] R. Foudazi, S. Qavi, I. Masalova, A.Y. Malkin, Physical chemistry of highly concentrated emulsions, Adv. Colloid Interface Sci. 220 (2015) 78–91.

[29] P.F. Luckham, M.A. Ukeje, Effect of Particle Size Distribution on the Rheology of Dispersed Systems, J. Colloid Interface Sci. 220 (1999) 347–356.

[30] S.M. Jafari, E. Assadpoor, Y. He, B. Bhandari, Re-coalescence of emulsion droplets during high-energy emulsification, Food Hydrocoll. 22 (2008) 1191–1202.

[31] D.J. McClements, J. Rao, Food-Grade nanoemulsions: Formulation, fabrication, properties, performance, Biological fate, and Potential Toxicity, Crit. Rev. Food Sci. Nutr. 51 (2011) 285–330.

[32] C. Chung, A. Sher, P. Rousset, D.J. McClements, Influence of homogenization on physical properties of model coffee creamers stabilized by quillaja saponin, Food Res. Int. 99 (2017) 770–777.

[33] N.M. Wiggers, H.J.; Zaioncz, S.; Cheleski, J.; Mainardes, R.M. and Khalil, Studies in Natural Products Chemistry, Elsevier Science, 2017.

[34] P. Riesz, D. Berdahi, C.L. Christman, Free radical generation by ultrasound in aqueous and nonaqueous solutions, 64 (1985) 233–252.

[35] L. Salvia-Trujillo, M.A. Rojas-Graü, R. Soliva-Fortuny, O. Martín-Belloso, Effect of processing parameters on physicochemical characteristics of microfluidized lemongrass essential oil-alginate nanoemulsions, Food Hydrocoll. 30 (2013) 401–407.

[36] M. Artiga-Artigas, A. Acevedo-Fani, O. Martín-Belloso, Effect of sodium alginate incorporation procedure on the physicochemical properties of nanoemulsions., Food Hydrocoll. 70 (2017) 191–200.

Figure 1. Particle size distribution**,** volume (d[4;3]) and surface (d[3;2]) mean droplet diameters and ζ-potential of highly concentrated ultrasonicated emulsions **(A, B** and **C**, respectively**)** or microfluidized emulsions **(D, E** and **F**, respectively**)** with a volume fraction of 0.4 and a surfactant-oil ratio of 0.1. Ultrasonication was performed during 20-300 s at 100 µm of amplitude and microfluidiation process was carried out during 1-5 cycles at 800 bar.

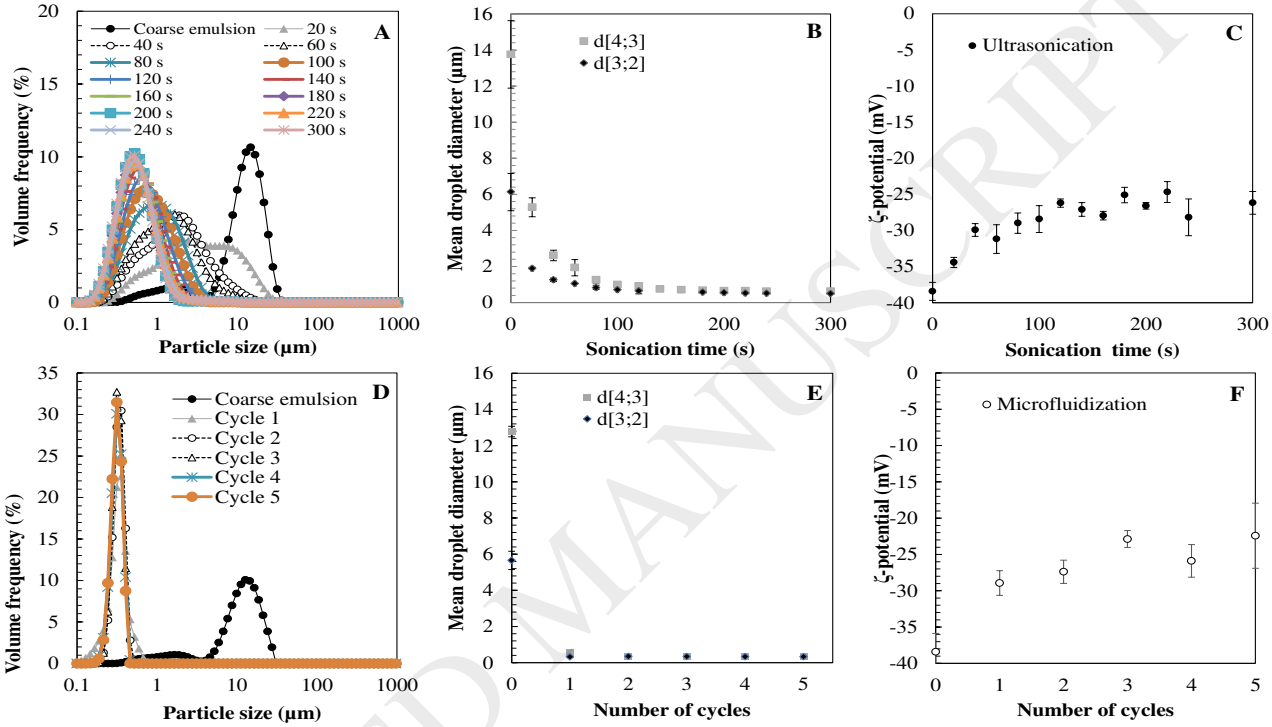

Figure 2. Particle size distributions of highly concentrated emulsions prepared by high-shear homogenization (11,000 rpm, 2 min) **(A)** and their subsequent submicron emulsions obtained by ultrasonication (100 µm, 200 s) **(B)** or microfluidization (800 bar, 2 cycles) **(C)** prepared with a surfactant-oil ratio of 0.1 and different volume fractions ranging from 0.4 to 0.7.

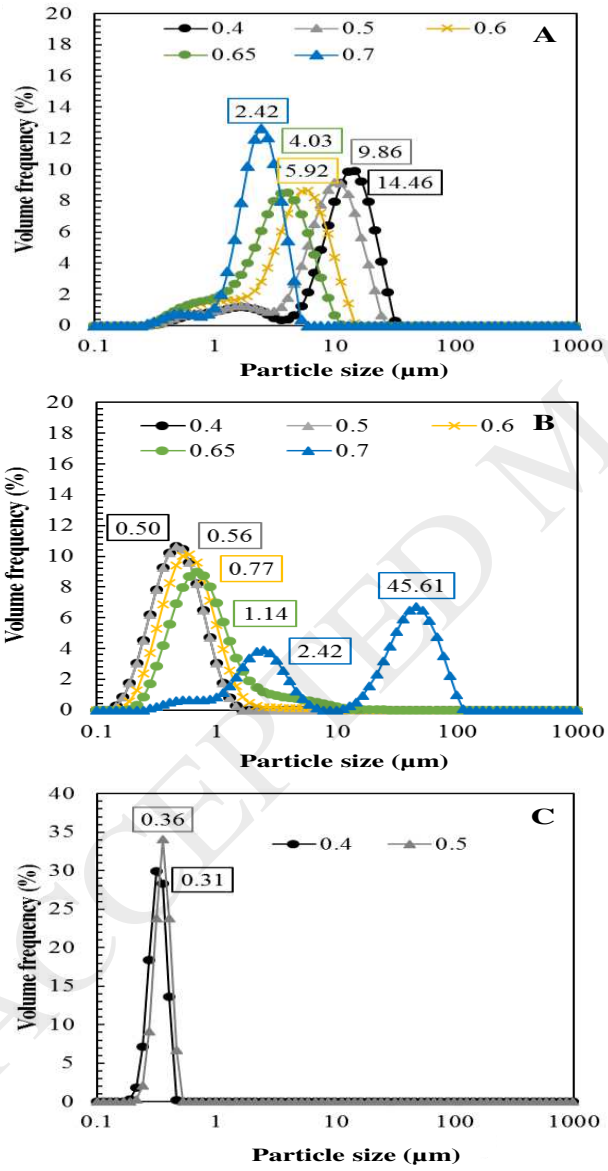

Figure 3. Microscopical phase contrast images of the highly concentrated emulsions prepared by high-shear homogenization (11,000 rpm, 2 min) **(A, D, G, J and M)** and their subsequent submicron emulsions obtained by ultrasonication (100 µm, 200 s) **(B, E, H, K and N)** or microfluidization (800 bar, 2 cycles) **(C, F, I and L)** prepared by a surfactant-oil ratio of 0.1 and volume fractions of 0.4-0.7. Error bar is equivalent a 20 µm. The image of microfluidized highly concentrated emulsion containing 0.7 as volume fraction is not reported since this sample could not been microfluidizes due to its high viscosity.

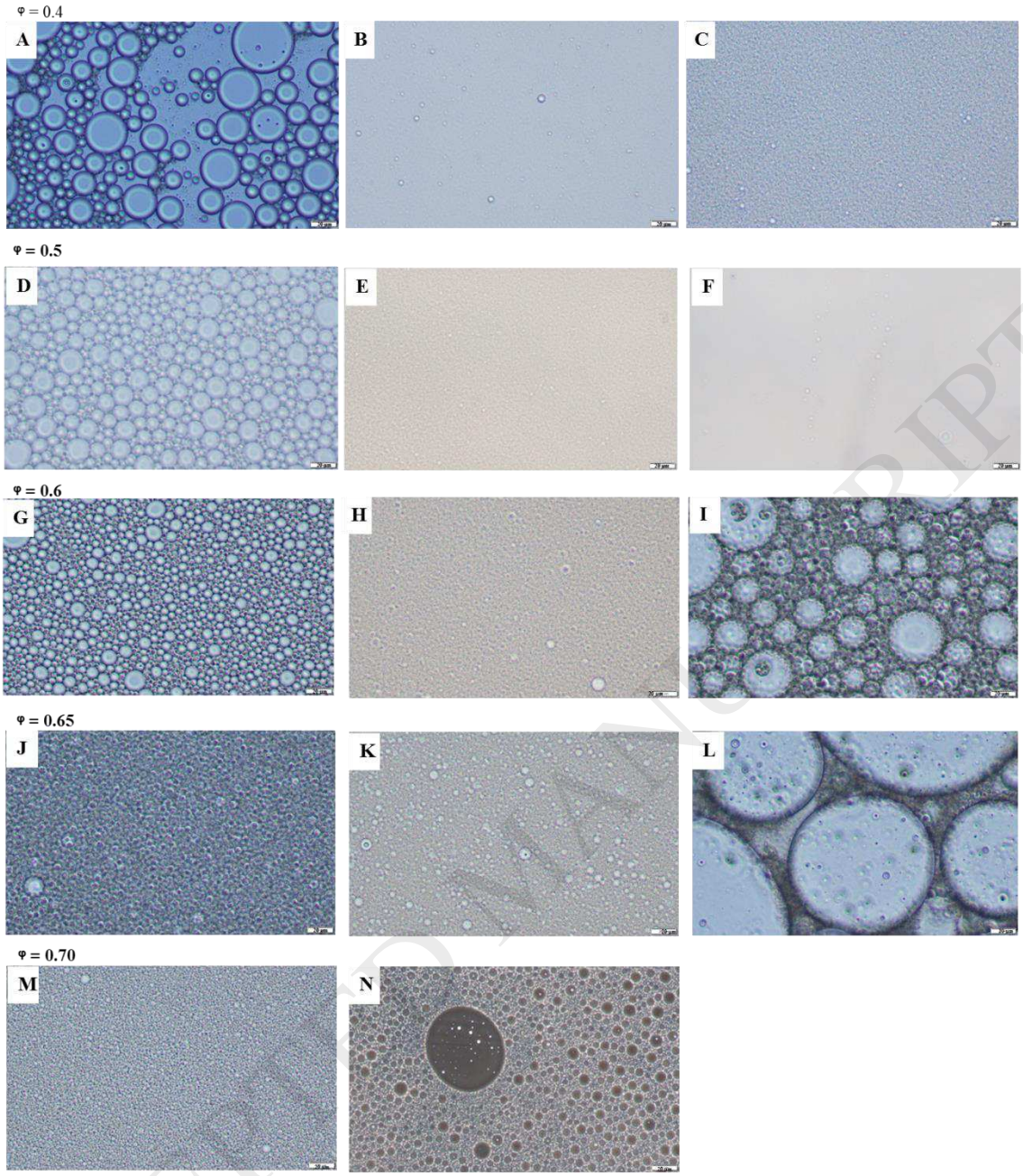

Figure 4. Influence of oil volume fraction (ϕ) on the particle size (full lines in µm) and on the apparent viscosity (grey bars in mPa·s) of highly concentrated emulsions produced by high shear homogenization at 11,000 rpm, 2 min **(A)**, ultrasonication at 100 µm, 200 s **(B)** and microfluidization at 800 bar, 2 cycles **(C)**.

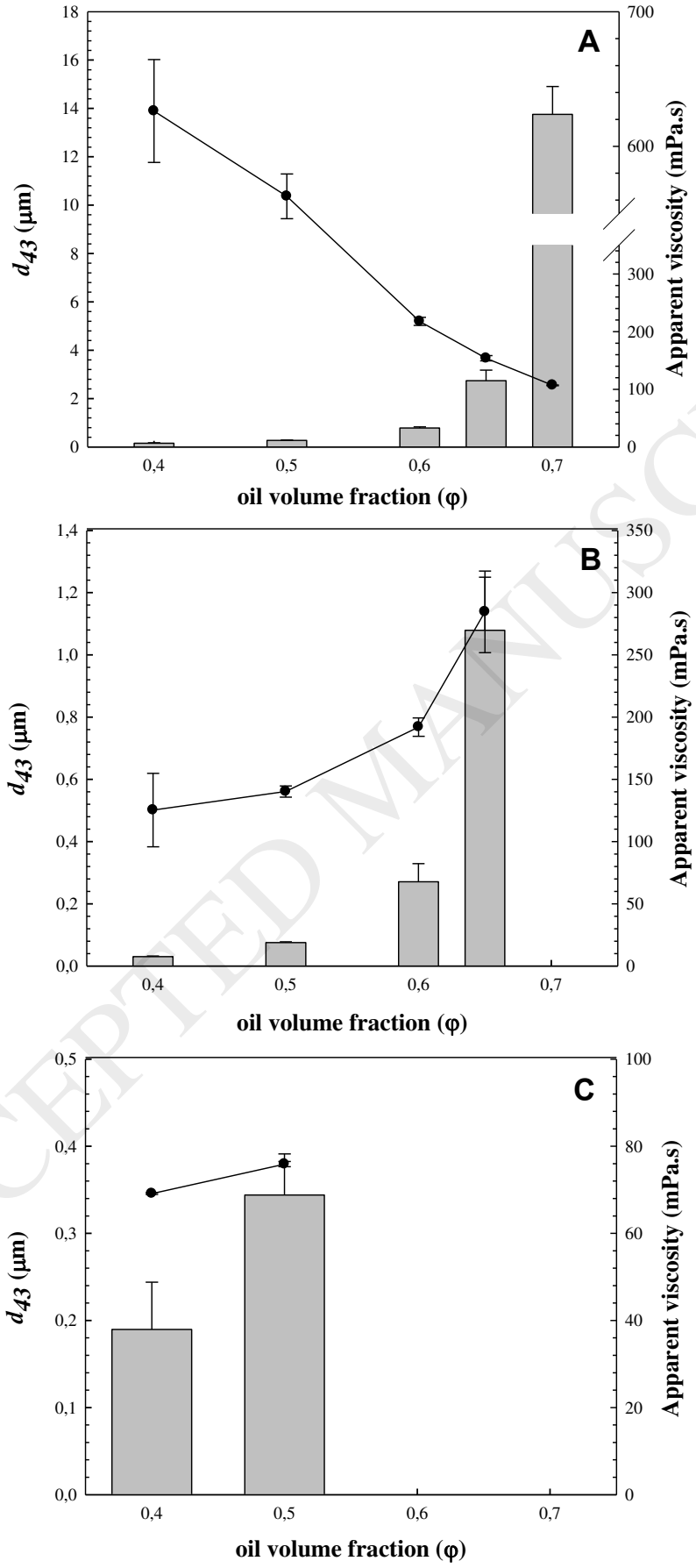

Figure 5. Particle size distributions of highly concentrated emulsions prepared by high-shear homogenization (11,000 rpm, 2 min) **(A)** and their subsequent submicron emulsions obtained by ultrasonication (100 µm, 200 s) **(B)** or microfluidization (800 bar, 2 cycles) **(C)** prepared with a volume fraction of 0.5 and different surfactant-oil ratio (0.01, 0.05, 0.07, 0.1 or 0.2).

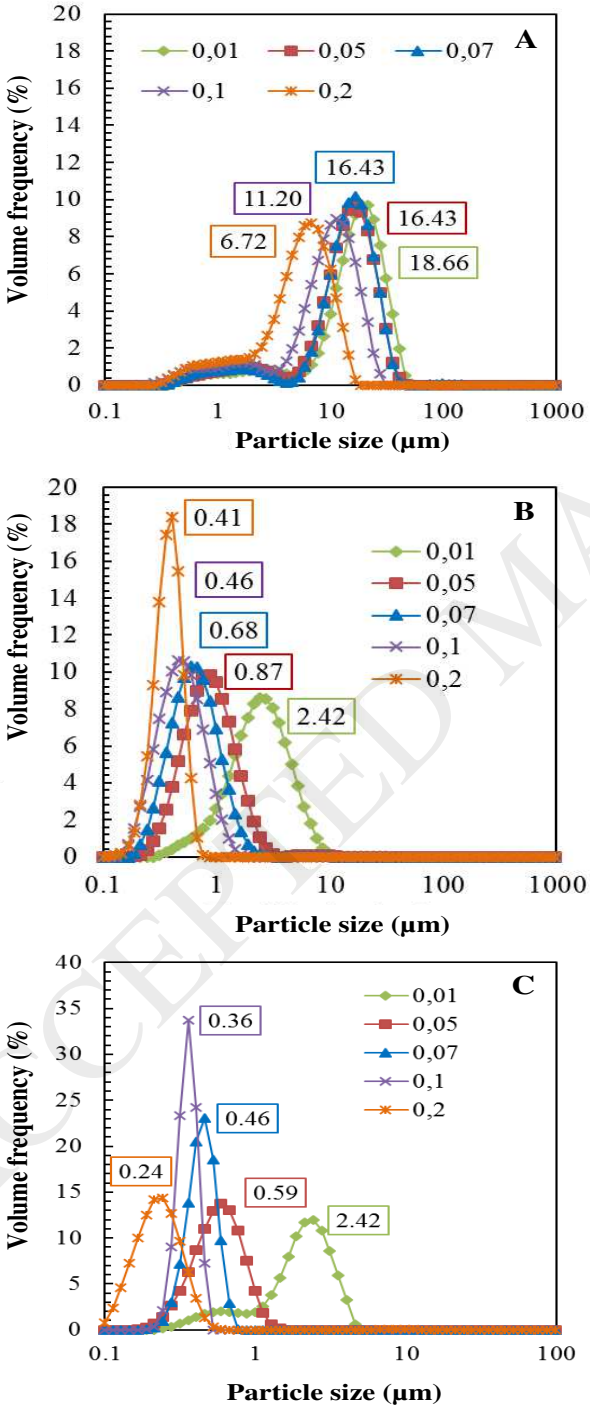

Figure 6. Microscopical phase contrast images of the highly concentrated emulsions prepared by high-shear homogenization (11,000 rpm, 2 min) **(A, D, G, J and M)** and their subsequent submicron emulsions obtained by ultrasonication (100 µm, 200 s) **(B, E, H, K and N)** or microfluidization (800 bar, 2 cycles) **(C, F, I, L and O)** prepared by a volume fraction of 0.5 and surfactant-oil ratios of 0.01, 0.05, 0.07, 0.1 or 0.2. Error bar is equivalent a 20 µm.

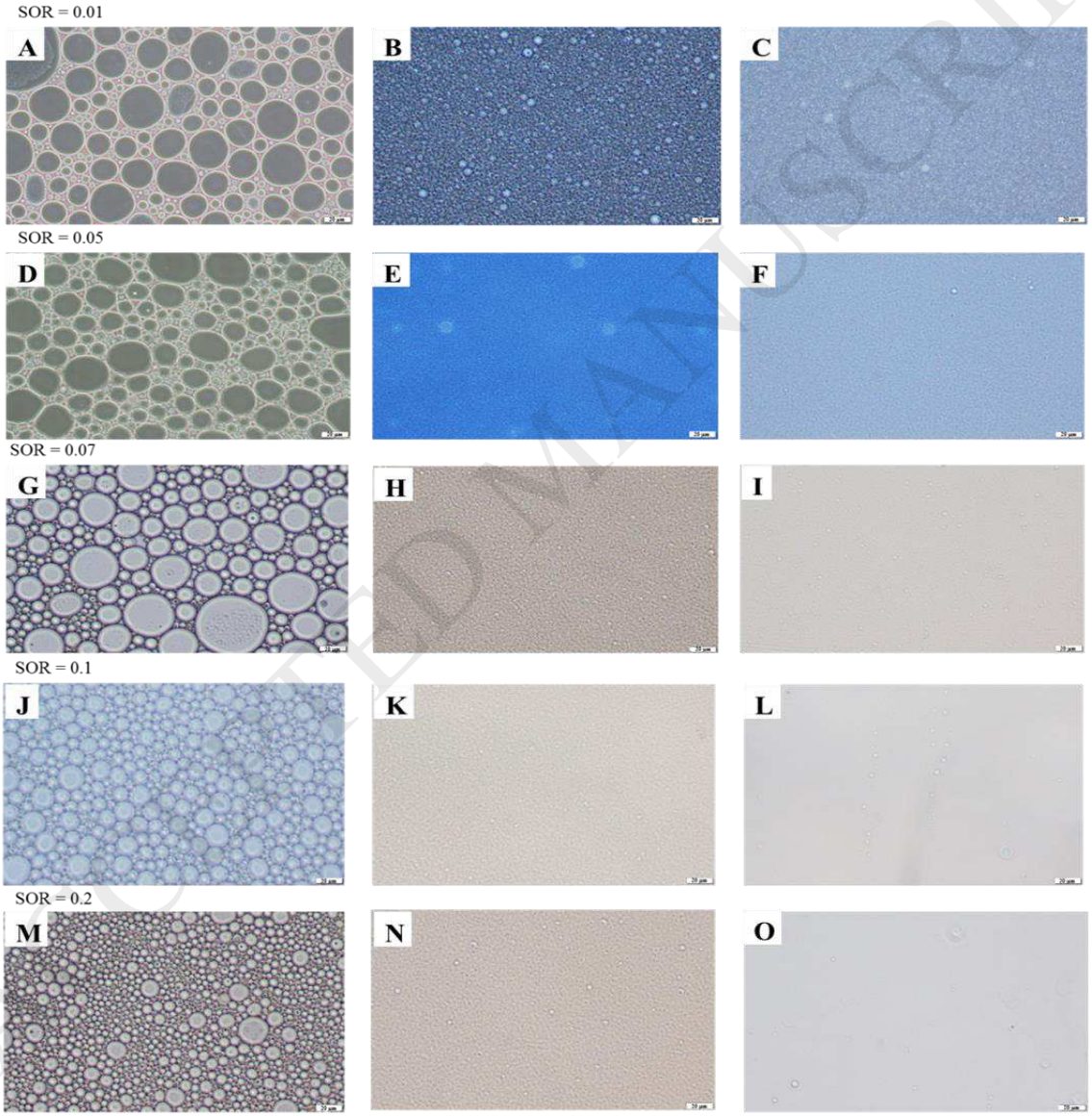

Figure 7. Surfactant to oil ratio (SOR) on the particle size (full lines in µm) and on the apparent viscosity (grey bars in mPa.s) of highly concentrated emulsions produced by high shear homogenization at 11,000 rpm, 2 min **(A)**, ultrasonication at 100 µm, 200 s **(B)** and microfluidization at 800 bar, 2 cycles **(C).**

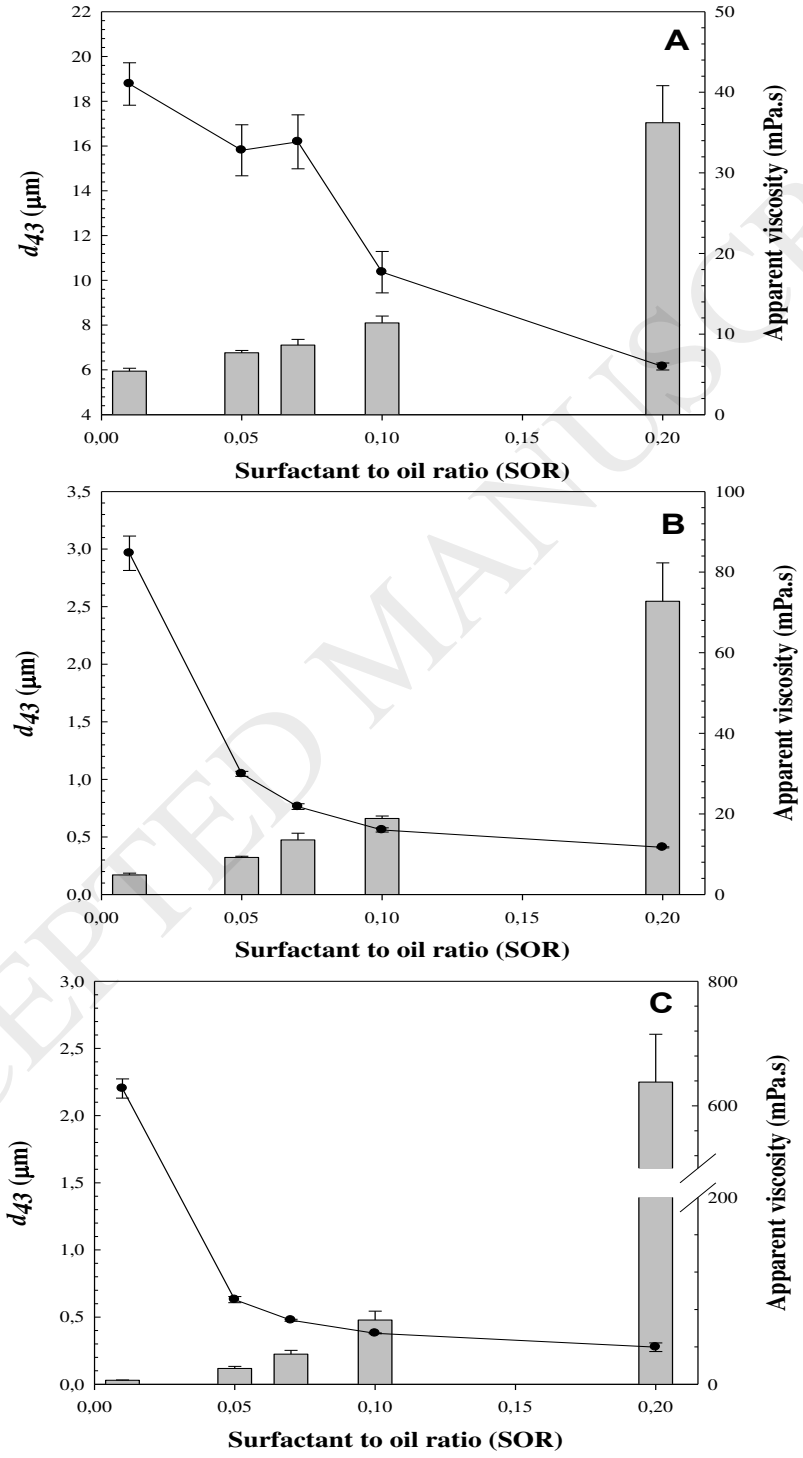

Figure 8. Curcumin release (%) of highly concentrated coarse emulsions prepared by high-shear homogenization (11,000 rpm, 2 min) and their subsequent submicron emulsions obtained by ultrasonication (200 s, 100 µm) or microfluidization (2 cycles, 800 bar) prepared with a surfactant-oil ratio of 0.1 and a volume fraction of 0.5. Emulsions were loaded with 0.01 % *w/w* of curcumin. The estimated maximum release (*CRmax*) expressed in % and the kinetic constant (k) in h^{-1} both calculated with the model: $CR = CRmax \cdot (1 - e^{-kt})$ are specified within the table.

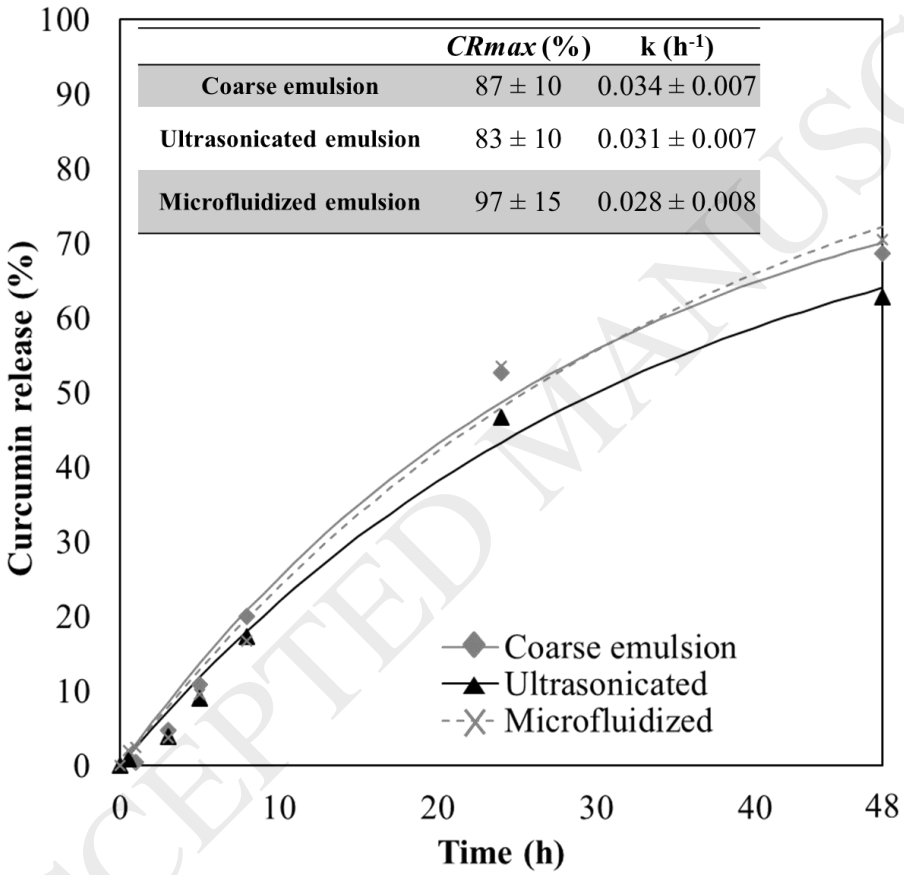

Table 1. ζ-potential (mV) and apparent viscosity (mPa·s) of high-shear homogenized, ultrasonicated (200 s, 100 μm) and microfluidized (2 cycles, 800 bar) highly concentrated emulsions with a SOR of 0.1, at different oil volume fractions (φ).

	φ	ζ-potential (mV)	Apparent viscosity (mPa·s)
High-shear homogenized emulsion	0.4	-37.9 ± 2.5 ^{ABb}	6.13 ± 0.73 ^{Da}
	0.5	-38.6 ± 2.1 ^{Bb}	11.7 ± 0.8 ^{Dc}
	0.6	-34.9 ± 2.8 ^{Ab}	33.3 ± 2.1 ^{Cb}
	0.65	-38.7 ± 1.9 ^{Bb}	115 ± 20 ^{Bb}
	0.7	-39.5 ± 2.6 ^{Bb}	624 ± 21 ^{Aa}
Ultrasonicated emulsion	0.4	-25.75 ± 1.26 ^{Ba}	7.84 ± 0.48 ^{Db}
	0.5	-21.43 ± 0.83 ^{Aa}	19.0 ± 0.7 ^{Cb}
	0.6	-20 ± 3 ^{Aa}	55.20 ± 0.27 ^{Ba}
	0.65	-28.9 ± 0.7 ^{Ba}	269 ± 52 ^{Aa}
	*0.7	-37.0 ± 2.6 ^{Cb}	33.1 ± 1.4 ^{Eb}
Microfluidized emulsion	0.4	-30 ± 2 ^{Ac}	28.1 ± 0.9 ^{Bb}
	0.5	-23.6 ± 1.52 ^{Ba}	63 ± 9 ^{Aa}
	*0.6		20 ± 0.5 ^{Ca}
	*0.65		23 ± 0.8 ^{Cc}

^{a,b,c} Means in same bar with different letters are significantly different at $p < 0.05$ regarding the φ. ^{A,B,C,D,E}Means in same bar with different letters are significantly different at $p < 0.05$ in terms of type of emulsion (high-shear homogenized, ultrasonicated or microfluidized). (*)Microfluidized emulsions containing $\varphi \geq 0.6$ destabilized after 1 cycle of microfluidization so their ζ-potential could not be measured and the reported apparent viscosity was measured after 1 cycle. Likewise, ultrasonicated emulsions with $\varphi = 0.7$ suffered disruption after ultrasonication.

Table 2. ζ-potential (mV) and apparent viscosity (mPa·s) of high-shear homogenized, ultrasonicated (200 s, 100 μm) and microfluidized (2 cycles, 800 bar) highly concentrated emulsions with a volume fraction of 0.5, at different surfactant-oil ratios (SOR).

	SOR	ζ-potential (mV)	Apparent viscosity (mPa·s)
High-shear homogenized emulsion	0.01	-52.6 ± 3.7 ^{Cc}	5.40 ± 0.37 ^{Ca}
	0.05	-47.11 ± 1.42 ^{Bc}	7.68 ± 0.29 ^{Cb}
	0.07	-40 ± 3 ^{Ab}	8.6 ± 0.7 ^{BCc}
	0.1	-42 ± 4 ^{Bc}	11.39 ± 0.84 ^{Bc}
	0.2	-37 ± 3 ^{Ac}	36 ± 5 ^{Ab}
Ultrasonicated emulsion	0.01	-44.1 ± 1.7 ^{Cb}	4.85 ± 0.43 ^{Dab}
	0.05	-25.38 ± 0.72 ^{Bb}	9.22 ± 0.28 ^{CDb}
	0.07	-25.1 ± 1.7 ^{Ba}	13.53 ± 1.68 ^{BCb}
	0.1	-21.9 ± 0.92 ^{Aa}	18.85 ± 0.63 ^{Bb}
	0.2	-25.00 ± 1.75 ^{Bb}	73 ± 9 ^{Ab}
Microfluidized emulsion	0.01	-40.2 ± 2.8 ^{Ca}	4.26 ± 0.38 ^{Cb}
	0.05	-20.1 ± 2.3 ^{Aa}	16.9 ± 2.3 ^{BCa}
	0.07	-25 ± 2 ^{Ba}	32 ± 4 ^{Bca}
	0.1	-27 ± 5 ^{Bb}	69 ± 9 ^{Ba}
	0.2	-22 ± 4 ^{Aa}	638 ± 77 ^{Aa}

^{A,B,C,D} Means in same bar with different letters are significantly different at $p < 0.05$ regarding the φ. ^{a,b,c} Means in same bar with different letters are significantly different at $p < 0.05$ in terms of type of emulsion (high-shear homogenized, ultrasonicated or microfluidized).